Hydrol. Earth Syst. Sci. Discuss., https://doi.org/10.5194/hess-2018-614
Manuscript under review for journal Hydrol. Earth Syst. Sci.
Discussion started: 22 January 2019

Hydrology and Earth System Sciences
Discussions

A Salinity Module for SWAT to Simulate Salt Ion Fate and Transport at the Watershed Scale

Ryan T. Bailey[1*], Saman Tavakoli-Kivi[1], Xiaolu Wei[1]

[1] Department of Civil and Environmental Engineering, Colorado State University, 1372 Campus Delivery, Fort Collins, CO, 80523-1372, United States.

[*]*Correspondence to*: Ryan Bailey (rtbailey@colostate.edu)

Abstract. Salinity is one of the most common water quality threats in river basins and irrigated regions worldwide. However, no available numerical models simulate all major processes affecting salt ion fate and transport at the watershed scale. This study presents a new salinity module for the SWAT model that simulates the fate and transport of 8 major salt ions (SO_4, Ca, Mg, Na, K, Cl, CO_3, HCO_3) in a watershed system. The module accounts for salt transport in surface runoff, soil percolation, lateral flow, groundwater, and streams, and equilibrium chemistry reactions in soil layers and the aquifer. The module consists of several new subroutines that are imbedded within the SWAT modelling code and one input file containing soil salinity and aquifer salinity data for the watershed. The model is applied to a 732 km^2 salinity-impaired irrigated region within the Arkansas River Valley in southeastern Colorado, and tested against root zone soil salinity, groundwater salt ion concentration, groundwater salt loadings to the river network, and in-stream salt ion concentration. The model can be a useful tool in simulating baseline salinity transport and investigating salinity best management practices in watersheds of varying spatial scales worldwide.

1 Introduction

Salinity is one of the most common water quality threats in river basins and irrigated regions worldwide. Sustainability of crop production in irrigated areas in semi-arid and arid areas is threatened by over-irrigation, poor quality of irrigation water (high salinity), inadequate drainage, shallow saline groundwater, and salinization of soil and underlying groundwater, all of which can lead to decreasing crop yield. Of the estimated 260 million ha of irrigated land worldwide, approximately 20-30 million ha (7-12%) is salinized (Tanji and Kielen, 2002), with a loss of 0.25 to 0.5 million ha each year globally. Approximately 8.8 million ha in western Australia alone may be lost to production by the year 2050 (NLWRA, 2001), and 25% of the Indus River basin is affected by high salinity. Within the western United States, 27-28% of irrigated land has experienced sharp declines in crop productivity due to high salinity (Umali, 1993; Tanji and Kielen, 2002), thereby rendering irrigated-induced salinity as the principal water quality problem in the semi-arid regions of the western United States.

Salinization of soil and groundwater systems is caused by both natural processes and human-made activities. Salt naturally can be dissolved from parent rock and soil material, with salt minerals (e.g. gypsum $CaSO_4$, halite NaCl) dissolving to mobile ions such as Ca^{2+}, SO_4^-, Na^+, and Cl^-. In addition, salt ions can accumulate in the shallow soil zone due to waterlogging, which is a result of over-irrigating and irrigating in areas with inadequate drainage. Salts moving up into the soil zone can become evapo-concentrated due to the removal of pure water by crop roots. Soil water salinization leads to a decrease in osmotic potential, i.e. the potential for water to move from soil to the crop root cells via osmosis, leading to a decrease in crop production.

Numerical models have been used extensively to assess saline conditions, simulate salt movement across landscapes and within soil profiles, predict salt build-up and movement in the root zone, and investigate the impact of best management practices (Oosterbaan, 2005; Schoups et al., 2005; Burkhalter and Gates, 2006; Singh and Panda, 2012). Available models that either have inherent salinity modules or can be applied to salinity transport problems include UNSATCHEM (Šimůnek and

Suarez, 1994), HYDRUS linked with UNSATCHEM (Šimůnek et al., 2012); DRAINMOD, LEACHC (Wagenet and Hutson, 1987), SAHYSMOD (Oosterbaan, 2005; Singh and Panda, 2012), CATSALT, and MT3DMS (Burkhalter and Gates, 2006).

Whereas several of these models include major ion chemistry for salt ions (e.g. precipitation-dissolution, cation exchange, complexation) (UNSATCHEM, HYDRUS), their application typically is limited to small field-scale or soil-profile domains (e.g. Kaledhonkar and Keshari, 2006; Schoups et al., 2006; Kaledhonkar et al., 2012; Rasouli et al., 2013). Conversely, models such as SAHYSMOD and MT3DMS have been applied to regional-scale problems, but lack the reaction chemistry and treat salinity as a conservative solute. SAHYSMOD uses seasonal water and salt balance components for large-scale systems on a seasonal time step (Singh and Panda, 2012). MT3DMS is a finite-difference contaminant transport groundwater model that uses MODFLOW output for groundwater flow rates, but does not include salt ion solution chemistry (Burkhalter and Gates, 2006). Schoups et al. (2005) used a hydro-salinity model that couples MODHMS with UNSATCHEM to simulate subsurface salt transport and storage in a 1,400 km^2 region of the San Joaquin Valley, California. The model, however, does not consider salinity transport in surface runoff or salt transport in streams, limiting results to soil salinity and groundwater. Currently, there is no model that simulates salt transport in all major hydrologic pathways (surface runoff, soil percolation and leaching, groundwater flow, streamflow) at the watershed-scale that also considers important solution reaction chemistry. Such a model is important for assessing watershed-scale and basin-scale salt movement and investigating the impact of large-scale salinity remediation schemes.

The objective of this paper is to present a salinity transport modeling code that can be used to simulate the fate and transport of the major ions (SO_4, Ca, Mg, Na, K, Cl, CO_3, HCO_3) in a watershed hydrologic system. The salinity module is implemented within the SWAT modeling code, and thereby salt transport pathways include surface runoff, percolation, soil later flow, groundwater flow and streamflow. The soil water and groundwater concentration of each salt ion is also affected by equilibrium chemistry reactions: precipitation-dissolution, complexation, and cation exchange. The use of the model is demonstrated through application to a 732 km^2 region of the Lower Arkansas River Valley (LARV) in southeastern Colorado, an irrigated alluvial valley in which soil and groundwater salinization has occurred over the past few decades. The model is tested against salt ion and total dissolved solids (TDS) concentration in surface water (Arkansas River and its tributaries), groundwater (from a network of monitoring wells), and soil water (from a large dataset of soil salinity measurements). The salinity module for SWAT can be applied to any watershed to simulate baseline conditions and to test the effect of best management practices on watershed salinity.

2 Development of the SWAT Salinity Module

This section provides a brief overview of the SWAT model, followed by a description of the SWAT salinity module. Sect. 3 demonstrates the use of the salinity module to a regional-scale irrigated stream-aquifer system in the Lowe Arkansas River Valley, Colorado.

2.1 The SWAT Model

The SWAT (Soil and Water Assessment Tool, Arnold et al., 1998) hydrologic model simulates water flow, nutrient mass transport and sediment mass transport at the watershed scale. It is a continuous, daily time-step, basin-scale, distributed-parameter watershed model that simulates water flow and nutrient (nitrogen, phosphorus) transport in surface runoff, soil percolation, soil later flow, groundwater flow and discharge to streams, and streamflow. The watershed is divided into subbasins, which are then further divided into multiple unique combinations (Hydrologic Response Units HRUs) of land use, soil type and topographic slope for which detailed water and nutrient mass balance calculations are performed. Routing algorithms route water and nutrient mass through the stream network to the watershed outlet. SWAT has been applied to hundreds of watersheds and

Hydrol. Earth Syst. Sci. Discuss., https://doi.org/10.5194/hess-2018-614
Manuscript under review for journal Hydrol. Earth Syst. Sci.
Discussion started: 22 January 2019

river basins worldwide to assess water supply and nutrient contamination under baseline conditions (Abbaspour et al., 2015) and scenarios of land use change (Zhao et al., 2016; Zuo et al., 2016; Napoli et al., 2017), best management practices (Arabi et al., 2006; Maringanti et al., 2009; Ullrich and Volk, 2009; Dechmi and Skhiri, 2013), and climate change (Jyrkama and Sykes, 2007; Ficklin et al., 2009; Tweed et al., 2009; Haddeland et al., 2010; Brown et al., 2015). However, it has not yet been applied to salinity issues.

2.2 Salinity Module for SWAT

The new SWAT salinity module simulates the fate and transport of 8 major salt ions (SO_4, Ca, Mg, Na, K, Cl, CO_3, HCO_3) via surface runoff, soil later flow, soil percolation and leaching, groundwater flow, and streamflow, subject to chemical reactions such as precipitation-dissolution, complexation, and cation exchange within soil layers and the alluvial aquifer. The module also simulates the loading of salt mass to the soil profile via saline irrigation water from both surface water (subbasin channel) and groundwater (aquifer) sources. A watershed cross-section schematic describing these processes is shown in Figure 1.

The salinity module is implemented directly into the SWAT FORTRAN code, with new subroutines developed for salt chemistry (*salt_chem*), salt irrigation loading (*salt_irrig*), salinity percolation and leaching (*salt_lch*), and salt groundwater transport and loading to streams (salt_gw). Other standard SWAT subroutines are modified to incorporate salt ion transport and effects, such as SWAT's crop growth modules, lagging solutes in surface runoff and groundwater flow (*surfstor*, *substor*), and routing solutes through the stream network (*watqual*). These subroutines are shown in Figure 2 within the general SWAT modeling code data flow. For each day loop, the mass balance calculations for each HRU are performed. Salt subroutines are shown for chemical equilibrium, irrigation loading, salt leaching, soil salinity stress, salt groundwater transport and loading, and lagging in surface runoff and groundwater flow. At the end of the HRU calculations, the water, sediment, nutrients, and salt mass is routed through the stream network, with in-stream concentration of each salt ion simulated for each SWAT subbasin. Details for each salt ion process are now presented. For the equations presented, *S* refers to salt mass, and the subscript *i* refers to the 8 major ions. For the transport equations, calculations are similar to SWAT's transport equations for nitrate. Salinity module input data and output data also will be discussed later in this section.

2.2.1 Salt in Surface Runoff ("salt_lch" and "surfstor" subroutines)

The mass of each salt ion can be transferred from an HRU to the subbasin channel via surface runoff. The salt ion mass generated in surface runoff $S'_{i,surf}$ (kg/ha) for the current day is calculated as:

$$S'_{i,surf} = \beta_{S_i} \cdot C_{S_i} \cdot Q_{surf} \quad (1)$$

where β_{S_i} is the salinity percolation coefficient, C_{S_i} is the concentration of the i^{th} salt ion in the mobile water for the top 10 mm of soil (kg salt /mm water), and Q_{surf} is the surface water generated from the HRU on a given day (mm water). As only a portion of the surface runoff and lateral flow reaches the subbasin channel on the day it is generated, SWAT uses a storage feature to surface runoff. The salt ion mass reaching the subbasin channel on the current day via surface runoff is calculated as:

$$S_{i,surf} = \left(S'_{i,surf} + S_{i,surfstor}\right) \cdot \left(1 - \exp\left[\frac{-surlag}{t_{conc}}\right]\right) \quad (2)$$

where $S_{i,surf}$ is the mass of the i^{th} salt ion that reaches the subbasin channel on the current day (kg/ha), $S_{i,surfstor}$ is the salt ion surface runoff stored or lagged from the previous day (kg/ha), *surlag* is the surface runoff lag coefficient, and t_{conc} is the time of concentration for the HRU (hrs).

2.2.2 Lateral Flow ("salt_lch" and "substor" subroutines)

The salt ion mass generated in lateral flow $S'_{i,lat,ly}$ (kg/ha) from a soil layer for the current day is calculated as:

$$S'_{i,lat,ly} = C_{S_i} \cdot Q_{lat,ly} \quad (3)$$

where $Q_{lat,ly}$ is the water discharge from the layer by lateral flow (mm water). Similar to surface runoff, only a portion of the lateral flow will reach the subbasin channel on the day it is generated, and thus the salt ion mass reaching the channel on the current day $S_{i,lat,ly}$ (kg/ha) via lateral flow is calculated as:

$$S_{i,lat,ly} = \left(S'_{i,lat,ly} + S_{i,latstor}\right) \cdot \left(1 - \exp\left[\frac{-1}{TT_{lat}}\right]\right) \quad (4)$$

where $S_{i,latstor}$ is the salt ion mass stored or lagged from the previous day (kg/ha) and TT_{lag} is the lateral flow travel time (days).

2.2.3 Soil Percolation ("salt_lch" subroutine)

The salinity module tracks the mass of each salt ion (kg/ha) in each soil layer. The salt ion mass moved to the underlying soil layer by percolation $S_{i,perc,ly}$ (kg/ha) is calculated as:

$$S_{i,perc,ly} = C_{S_i} \cdot Q_{perc,ly} \quad (5)$$

where $Q_{lat,ly}$ is the amount of water percolating to the underlying soil layer on a given day (mm water). After percolation has been simulated, the concentration of each salt ion (mg/L) in each soil layer is calculated using the area (m^2) of the HRU and the volume of water in the soil layer (m^3). The leached salt ion mass is added to the shallow aquifer using the following:

$$S_{i,rech} = \left[\left(1 - gw_{delay}\right) \cdot S_{i,perc}\right] + \left(gw_{delay} \cdot S_{i,rech,t-1}\right) \quad (6)$$

where $S_{i,rech}$ is the salt ion mass loaded to the water table via recharge (kg/ha), $S_{i,perc}$ is the salt ion mass percolated from the bottom layer of the soil profile, $S_{i,rech,t-1}$ is the leached salt ion mas from the previous day, and gw_{delay} is the groundwater delay time, i.e. the time required for water leaving the bottom of the root zone to reach the water table (days).

2.2.4 Groundwater Flow ("salt_gw" subroutine)

The salinity module tracks the mass of each salt ion (kg/ha) in the aquifer. The salt ion mass generated in groundwater flow $S'_{i,gw}$ (kg/ha) from the aquifer for the current day is calculated as:

$$S'_{i,gw} = C_{S_{i,gw}} \cdot Q_{gw} \quad (7)$$

where $C_{S_{i,gw}}$ is the salt ion concentration in the aquifer (kg salt /mm water), and Q_{gw} is the groundwater flow generated for the HRU for the current day (mm water). The concentration of each salt ion in each HRU aquifer is calculated on each day by dividing the total mass of the salt ion (g) by the total volume of groundwater (m^3).

2.2.5 Streamflow ("watqual" subroutine)

Water is routed through the watershed channel network using the variable storage routing method, a variation of the kinematic wave model (Neitsch et al., 2011). The mass of each salt ion is routed through the channel network with water, with no chemical reactions changing in-stream salt ion concentration. Similar to any constituent in SWAT, salt ion loadings (kg/day) can be specified for any subbasin reach of the watershed.

2.2.6 Salt Loading in Irrigation water ("salt_irrig" subroutine)

Salt ion mass is added to the soil profile via irrigation water, with water derived from either the aquifer (groundwater pumping) or from surface water diversions. Including constituent mass in irrigation water is a new feature for SWAT, as the original code does not account for nutrient (N, P) mass in irrigation water. If the irrigation water source is a subbasin reach (surface water irrigation), the concentration of each salt ion is multiplied by the volume of applied irrigation water (depth of water * HRU area) to determine the mass of each salt ion (kg/ha) to add to the first soil layer. If the irrigation water source is the

shallow aquifer, the concentration of each salt ion in the HRU aquifer is used to estimate salt loading to the first soil layer. The salt ion mass is then removed from the HRU aquifer.

2.2.7 Salt Solution Chemistry

The salinity chemistry implemented into SWAT is based on the Salinity Equilibrium Chemistry (SEC) module developed for soil-aquifer systems (Tavakoli-Kivi, 2018). The equations for salinity solution chemistry presented here are performed for each HRU soil layer and for each HRU. The solution chemistry in this module is similar to that implemented in other water chemistry models [UNSATCHEM: Šimůnek et al. (2012), PHREEQC: Parkhurst and Appelo (2013), MINTEQA2: Paz-Garcia et al. (2013)]. Thus, only basic details are presented here.

The SEC module includes 8 aqueous components, 10 complexed species, five solid (salt mineral) species, and four exchange species (Table 1). The 8 aqueous components (SO_4, Ca, Mg, Na, K, Cl, CO_3, HCO_3) are included due to their presence in the majority of soil-aquifer systems. The five salt minerals ($CaSO_4$, $CaCO_3$, $MgCO_3$, NaCl, $MgSO_4$) also are included due to their presence in many soil-aquifer systems, although the module can be amended to include any mineral species. The module simulates the dissolved concentration (mg/L) of the 8 ions in soil water and groundwater and the solid mass concentration of the five salt mineral species in the soil and the aquifer sediment according to precipitation-dissolution, complexation, and cation exchange reactions.

For these calculations, the duration of the model time step (daily time step for SWAT) is assumed long enough for all constituent reactions to achieve equilibrium. The concentration of species at equilibrium is calculated using a stoichiometric algorithm approach, in which mass balance and mass action equations are solved simultaneously. This method is used in other water chemical equilibrium packages such as PHREEQC (Parkhurst and Appelo, 2013) and MINTEQA2 (Paz-Garcia et al., 2013).

Law of Mass Action

At equilibrium, the concentration of all reactants and products are related using the equilibrium constant K:

$$K = \frac{(\mathrm{C})^c(\mathrm{D})^d}{(\mathrm{A})^a(\mathrm{B})^b} \quad (8)$$

where A and B are reactants, C and D are reactants, a, b, c, and d are constants, and the parentheses denote solute activities. The activity of the i^{th} solute, i_A, is computed by multiplying the activity coefficient γ_i by the molal concentration, where γ_i depends on the ionic strength I of the solution:

$$I = \frac{1}{2}\sum m_i . z_i^2 \quad (9)$$

where z_i is the charge number of the i^{th} ion and mi is the molality (mol/kg H_20). γ_i is then given as:

$$\begin{cases} \log\gamma_i = -\dfrac{A_a z_i^2\sqrt{I}}{1+B_a a_i\sqrt{I}} & I < 0.1 \\ \log\gamma_i = -Az_i^2\left(\dfrac{\sqrt{I}}{1+\sqrt{I}} - 0.3I\right) & 0.1 < I < 0.5 \end{cases} \quad (10)$$

where A_a and B_a are temperature dependent constants (A_a = 0.5085 m^{-1} and $B_a = 0.3285\times10^{10}$ m^{-1} at 25° C) and a_i is a measure of effective diameter of a hydrated ion i. The first equation in (10) is the Debye-Huckle equation for dilute solutions, and the second equation is the Davis equation.

Mass Balance Equations

The mass of each element in the system, either in ion or complexed form, is tracked by a set of mass balance equations. Equations for SO_4, Cl, Ca, and Na are:

Hydrol. Earth Syst. Sci. Discuss., https://doi.org/10.5194/hess-2018-614
Manuscript under review for journal Hydrol. Earth Syst. Sci.
Discussion started: 22 January 2019

Hydrology and Earth System Sciences
Discussions

$$SO_{4_T}=[SO_4^{2-}]+[CaSO_4^0]+[MgSO_4^0]+[NaSO_4^-]+[KSO_4^-] \quad (11a)$$

$$Cl_T=[Cl^-] \quad (11b)$$

$$Ca_T=[Ca^{2+}]+[CaSO_4^0]+[CaCO_3^0]+[CaHCO_3^+] \quad (11c)$$

$$Na_T=[Na^+]+[NaSO_4^-]+[NaCO_3^-]+[NaHCO_3^0] \quad (11d)$$

where *T* denotes total concentration and brackets indicate species' molality. Similar equations are written for Mg, K, CO_3, and HCO_3.

Precipitation-Dissolution Reactions

Salt minerals (AB_s) can dissolve or precipitate according to the stoichiometric reaction

$$AB_s \leftrightarrow A^+_{aq} + B^-_{aq} \quad (12)$$

The salt mineral will dissolved if the solution is under-saturated in in regards to A^+_{aq} and B^-_{aq}, and will precipitate if the solution is super-saturated. Salt minerals in the SEC module include $CaSO_4$, $CaCO_3$, $MgCO_3$, $MgSO_4$, and NaCl, due to their common occurrence in aquifers. For example:

$$CaSO_4 \leftrightarrow Ca^{2+} + SO_4^{2-} \quad (13)$$

with a solubility product constant:

$$K_{sp_{CaSO_4}} = \frac{(Ca^{2+})(SO_4^{2-})}{(CaSO_4)} \quad (14)$$

Within the SEC module, minerals are added to the system one at a time, with the solubility limits of each mineral used to determine the direction of each reaction (precipitation or dissolution).

Complexation Reactions

Based on the law of mass action, equilibrium equations are written for all complexed species. For example, the equation for $CaSO_4^0$ is:

$$K_{CaSO_4} = \frac{(Ca^{2+})(SO_4^{2-})}{CaSO_4^0} \quad (15)$$

where K_{CaSO_4} is the equilibrium constant and is equal to 0.004866. Equations and equilibrium constants for the remaining 9 complexed species are shown in Supporting Material.

Cation Exchange Reactions

Cation exchange is calculated to determine the sorbed and released ions from sediment surfaces to the solution. The order of replaceability is Na > K > Mg > Ca, determined by Coulomb's Law. The cation reaction as an equivalent reactions represented by Gapon equation:

$$X_{1/mM} + 1/n\ N^{n+} = X_{1/nN} + 1/m\ X^{m+} \quad (16)$$

where $X_{1/mM}$ is exchangeable cation *M* on the surface (meq/100), $X_{1/nN}$ is exchangeable cation *N* on the surface (meq/100g), *M* and *N* are metal cations, and *m*+ and *n*+ are the charges of cations *M* and *N* respectively. Using the cation exchange capacity of the soil and a coefficient of Gapon selectivity coefficient for each reaction, concentration of each exchangeable species is determined.

2.2.8 Salinity Module Input/Output

Required data for running the SWAT salinity module include: precipitation-dissolution solubility products for the five salt minerals ($CaSO_4$, $CaCO_3$, $MgCO_3$, NaCl, $MgSO_4$), initial concentration of salt ions in soil water and groundwater, and initial salt mineral solid concentration (% of bulk soil) in soil and aquifer sediment. Initial concentrations are required for each HRU. However, as will be shown in Sect. 3, using uniform (i.e. all HRU values are the same) concentration values yields the same result as using spatially-variable initial concentrations, if a warm-up period of several years is used in the SWAT simulation.

All input data are provided in a single input file, "*salt_input*". To turn on the salinity module, a single line has been added at the end of the *file.cio* file, with flag being read (0 or 1) to exclude/include the salinity module. If the flag is set to 1, the SWAT code will open and read the contents of the *salt_input* file.

3 Application of SWAT Salinity Module to an Irrigated Stream-Aquifer System

3.1 Study Region: Lower Arkansas River Valley, Colorado

The salinity module is tested for a 732 km^2 irrigated stream-aquifer system along the Arkansas River in southeastern Colorado (Figure 3A). The region consists the Arkansas River and tributaries (e.g. Timpas Creek, Crooked Arroyo, see Figure 3A) running through and over a thin (~10-15 km in width) and shallow (~10-20 m) sandy alluvial aquifer. The climate is semi-arid, requiring irrigation to supplement rainfall for crop growth. Irrigation water is derived either from the Arkansas River via a system of irrigation canals or from the aquifer via a network of ~500 pumping wells (Figure 3A). Cultivation and associated irrigation occurs March through November.

Salinization of soil, groundwater, and surface water in the region has steadily worsened since the 1970s due to increased irrigation diversions from the Arkansas River, high water tables due to excessive water applications to fields, and the existence of salt minerals, particularly gypsum ($CaSO_4$) (Konikow and Person, 1985; Goff et al., 1998; Gates et al., 2002; Gates et al., 2016). Soil salinity levels under about 70% of the area exceed threshold tolerance for crops, with the regional average of crop yield reduction from salinity and waterlogging estimated to range from 11 to 19% (Gates et al., 2002; Morway and Gates, 2012).

From sampling groundwater from a network of 82 observation wells (see Figure 3B) (sampling from June 2006 to May 2010), average salinity concentration of shallow groundwater is approximately 2,700 to 3,000 mg/L, and annual salt loading to the Arkansas River from groundwater return flows is about 500 kg per irrigated ha, per km of the river. In the 1990s, 68% of producers stated that high salinity levels are a significant concern (Fraser et al., 1999). For the region modeled in this study, average TDS concentration (C_{TDS}) in groundwater is 3,334 mg/L (443 samples), with a minimum of 459 mg/L and a maximum of 44,600 mg/L. The presence of gypsum is revealed in the high concentration of SO4 (C_{SO_4}), with average, minimum, and maximum concentrations of 1,878 mg/L, 147 mg/L, and 29,457 mg/L, respectively. Average soil salinity, using electrical conductivity (EC), is 4.11 dS/m (54,700 measurements), with minimum and maximum of 0.9 dS/m and 56.5 dS/m, respectively. Based on 6 surface water sampling sites (4 in the Arkansas River, 2 in tributaries; Figure 3B), average C_{TDS} and C_{SO_4} is 1145 mg/L and 560 mg/L, respectively. More details of observed groundwater, soil water, and surface water concentrations are provided in Sect. 3.3.2 when model results are presented.

3.2 SWAT Model

A previously calibrated and tested SWAT model for the study region is used to simulate salt fate and transport using the developed salinity module. The SWAT model is detailed in Wei et al. (2018). The region was divided into 72 subbasins (see Figure 3B). A method was developed to apply SWAT to highly-managed irrigated watersheds, and included: designating each cultivated field as an individual HRU (see Figure 3B for the map of fields); crop rotations to simulate the effects of changing

crop types for each field during the 11-year simulation; seepage to the aquifer from the earthen irrigation canals; and SWAT's auto-irrigation algorithms to trigger irrigation events based on plant water demand for both surface water irrigation and groundwater irrigation. The method resulted in 5,270 HRUs. Implementing canal seepage required a slight change to the SWAT modeling code to add pre-processed, estimated canal seepage to HRU aquifer. Canal seepage rates were obtained from field measurements (Susfalk eta l., 2008; Martin et al., 2014). The model was run for the 1999-2009 time period, with simulated streamflow compared to observed hydrographs at 5 stream gages (Rocky Ford, La Junta, Las Animas, Timpas Creek, Crooked Arroyo; see Figure 3B) for model testing (Wei et al., 2018).

3.3 SWAT Model with Salinity Module

3.3.1 Model Construction and Simulation

The SWAT model is run from April 1 1999 to December 13 2009, with observed data for testing available from June 2006 to December 2009. The 1999-2005 period thus serves as a warm-up simulation period. The calibration period is 2006-2007, and the testing period from 2008-2009. Required inputs include initial soil water and groundwater ion concentrations, initial soil and aquifer sediment salt mineral fractions and, due to the study region being a part of the larger Lower Arkansas River Valley, ion mass loading in the Arkansas River at the upstream end of the modeled region (Catlin Dam; see Figure 3B).

Salt ion mass loading (kg/day) in the Arkansas River at Catlin Dam were estimated using daily measured values of EC (dS/m) and streamflow (m^3/s) and periodic measurements of salt ion concentration (mg/L). Linear relationships were established between EC and the concentration of each salt ion, with this relationship then used to estimate salt ion concentration for each day of the simulation period. The daily in-stream mass of each salt ion was then calculated by multiplying daily salt ion concentration by streamflow, and added to the point-source SWAT input file for the appropriate subbasin. Figure 4A shows the daily loading (kg/day) for each salt ion using this method. The make-up of total mass loading by salt ion is shown in Figure 4B, with SO_4 accounting for 47% of total in-stream salt mass. The linear relationship between EC and selected salt ions (SO_4, Cl, Na) and TDS is shown in the charts along the bottom of Figure 4. For TDS the R^2 value of the relationship is approximately 0.93.

Initial salt ion concentrations in soil water and groundwater were based on averages of observed groundwater concentrations. For the baseline simulation, the same values were assigned to each HRU. These are 1875 mg/L, 330 mg/L, 175 mg/L, 440 mg/L, 10 mg/L, 150 mg/L, 5 mg/L, and 350 mg/L for C_{SO_4}, C_{Ca}, C_{Mg}, C_{Na}, C_K, C_{Cl}, C_{CO_3}, and C_{HCO_3}, respectively. The effect of using spatially-varying initial concentrations is explored in additional scenarios. Salt mineral fractions for $CaSO_4$ and $CaCO_3$ in the HRU soil layers are based on a soil survey of the region from the Natural Resources Conservation Service (NRCS). The fraction of soil that is $CaSO_4$ and $CaCO_3$ was set to 0.1 and 0.01. For the aquifer sediment, fractions are based on the spatial patterns determined in Tavakoli-Kivi (2018) for a salinity groundwater transport study of the same region. Solubility products for precipitation-dissolution of salt minerals were obtained from literature and from Tavakoli-Kivi (2018) and are 3.07×10^{-9}, 4.8×10^{-6}, 4.9×10^{-5}, 0.0072, and 37.3 for $CaCO_3$, $MgCO_3$, $CaSO_4$, $MgSO_4$, and NaCl, respectively, for both soil and aquifer sediments.

Only minimal manual calibration was applied to the model, to yield correct magnitudes of salt ion concentration in soil water, groundwater, and stream water. Targeted parameters were the solubility product of $CaSO_4$ precipitation-dissolution, and the soil fraction of $CaSO_4$. The solubility produce was increased from 0.000049 to 0.0003, and the soil fraction of $CaSO_4$ was decreased from 0.01 to 0.009. Model results are tested against in-stream concentration of salt ions, soil water EC (dS/m), groundwater concentration of salt ions, and groundwater salt ion mass loading to the Arkansas River. Observed soil EC values were obtained using a saturated paste extract, and hence comparison with model results will not be as rigorous as for groundwater and surface water data.

Several variations of the model were run to test the effect of 1) initial salt ion concentrations and 2) specified loading of salt ion mass at the upstream end of the Arkansas River. For 1), the variations include uniform initial concentrations (baseline model), random spatially-variable concentrations, and initial concentrations equal to 0. For 2), the variation included one simulation with no loading.

3.3.2 Model Results

Model results consist of in-stream salt ion and TDS concentration, hydrologic pathway (groundwater discharge, surface runoff, percolation) salt loadings, groundwater salt ion concentration, soil water EC, watershed-wide salt balance, and groundwater salt loading to the Arkansas River.

3.3.2.1 In-Stream Salt Ion Concentration

Simulated and observed in-stream salt ion concentrations (mg/L) are shown in Figure 5 for the Rocky Ford site (Figure 5A) and the Crooked Arroyo site (Figure 5B). Results are shown for SO_4, Ca, Cl, and HCO_3, with the calculated Nash-Sutcliffe model efficiency coefficient (NSE) shown on each plot. Results for TDS at all 5 gaging stations are shown in Figure 6. As can be seen by the trends in concentration and also the NSE values, the SWAT model performs well in replicating in-stream salt ion concentrations, particularly for SO_4 (NSE = 0.60), Ca (NSE = 0.54), HCO_3 (NSE = 0.73), and TDS (NSE = 0.69) in the Arkansas River at the Rocky Ford gaging site. The model does not perform as well in downstream sites, with NSE at La Junta and at Las Animas equal to 0.34 and 0.25, respectively, although the trends are correct and the magnitudes are correct except for at the downstream-most site (Las Animas), where the model under-predicts total salt concentration. This is also shown by a 1:1 comparison of all salt ion data for the Rocky Ford (Figure 7A) and Las Animas (Figure 7C) sites, which yield R^2 values of 0.87 and 0.74, respectively. Las Animas also has an R^2 value of 0.74. However, as the SWAT model often is used to estimate monthly in-stream loads rather than daily in-stream concentration, these results are promising regarding the use of SWAT to estimate in-stream salinity loadings.

In regards to the NSE, the model performs rather poorly in the two tributaries (Timpas Creek, Crooked Arroyo), with NSE equal to -0.32 and 0.41, respectively, for TDS (Figure 6B, 6C). However, the overall trends and magnitude compare well to observed data. This is shown in the 1:1 plot of all salt ion data for Timpas Creek in Figure 7B, resulting in an R^2 value of 0.79. The relationship for Crooked Arroyo yields an R^2 value of 0.80. This is particularly promising given that there is no specified upstream loading for the tributaries, and hence all salt mass within the stream system is due to surface runoff, lateral flow, and groundwater discharge. Hence, comparing simulated and observed in-stream salinity concentration in these two systems is a strong test for the model.

Figure 8 shows the salt loading via the hydrologic pathways of groundwater discharge (Figure 8A), surface runoff (8B), and percolation from the soil profile to groundwater (8C). For Timpas Creek, 96% of salt in the creek water is from groundwater discharge, 3% from surface runoff, and 1% from lateral flow. For Crooked Arroyo, the portions are 91%, 6%, and 3%, and for the Arkansas River they are 96%, 3%, and 1%, highlighting the strong influence of groundwater on surface water salt load. This is shown further by examining the domain-wide salt balance, presented in Sect. 3.3.2.3. The mass loading of total salt from the aquifer to the Arkansas River for each day of the 2006-2009 time period is shown in Figure 9. Mass balance plot values are the mean of a a stochastic river mass balance calculation of surface water salinity loadings along the length of the Arkansas River within the model domain, using a method similar to Mueller-Price and Gates (2008), with values indicating the mass of salt not accounted for by surface water loadings. These unaccounted for loadings include groundwater, and thus provide an upper limit of in-stream salt loading from groundwater discharge.

340 **3.3.2.2 Groundwater and Soil Water Salinity**

341 Groundwater salt results are shown by spatial maps and by comparison of frequency distributions. For all simulated results,
342 only concentration values from days on which field samples were taken are included in the analysis. Time-averaged TDS (mg/L),
343 SO_4 (mg/L), and Na (mg/L) in groundwater is shown for each HRU in Figure 10. Also shown is soil water EC (dS/m) for each
344 HRU soil profile, and the percent of the soil profile (Figure 10E) and aquifer (Figure 10F) that is $CaSO_4$ (solid mineral) at the
345 end of the simulation period. These maps are shown to provide an indication of the degree of spatial variation simulated by the
346 salinity module. Variation in each system response is large, with TDS ranging from 0 to ~11,700 mg/L, SO_4 from 0 to ~6700
347 mg/L, and Na from 0 to ~1,270 mg/L. In comparison, if data from an outlier monitoring well are excluded (monitoring well with
348 salinity values more than double of any other monitoring well), the maximum observed values for TDS, SO_4, and Na are 13,000
349 mg/L, 6,500 mg/L, and 2,600 mg/L.

350 Results for all salt ions are summarized in Table 2. Average concentration of field samples (based on field samples from 82
351 monitoring wells shown in Figure 3B) and HRU-simulated groundwater salinity compares well, particularly for SO_4 (1,878 mg/L
352 to 2,058 mg/L) and for TDS (3,334 mg/L to 3,276 mg/L). In addition to a comparison of maximum and average values,
353 comparison at various magnitude levels is performed using relative frequency plots, shown in Figure 11. Results for SO_4 (Figure
354 11A), HCO_3 (11B), and TDS (11C) are shown. Similar to the results shown in Table 2, the comparison for SO_4 and TDS is good,
355 but the model generally under-predicts HCO_3 for most HRUs. A relative frequency plot of observed and simulated EC (dS/m) in
356 the soil profile also is shown (Figure 11D). The average of observed values and simulated values are 4.1 dS/m and 4.8 dS/m,
357 although the majority of observed values are between 2 dS/m and 4 dS/m whereas no such grouping occurs for the simulated
358 values. However, the observed data values are obtained from saturated paste extracts, which therefore lowers the salinity
359 concentration due to the addition of water to bring the soil to saturation. Hence, the "observed" (modified by the saturated paste
360 method) concentrations should be lower than what actual occurs in the field, which may explain the disagreement shown in
361 Figure 11D.

362 **3.3.2.3 Salt Balance**

363 The domain-wide salt balance is presented in Figure 12A. All salt balance components are included, with all values scaled
364 according to the small salt flux (lateral flow = 1 unit). For the soil profile, salt is added via groundwater irrigation (12 units),
365 surface water irrigation (33), dissolution of salt minerals (110), and upflux from the aquifer saturated zone (39), and removed via
366 percolation (103), surface runoff (4), and lateral flow (1). A similar salt balance can be performed for each salt ion in the system.
367 Salt removed from the aquifer and added to the soil profile via upflux is approximately 30% of percolation, which compares well
368 to a comparison of water upflux and recharge magnitudes computed by Morway et al. (2013) in a groundwater modeling study of
369 the region using MODFLOW.

370 Of the salt entering the river, 96.7% is from groundwater (151 units out of 156), and the remaining from surface runoff and
371 lateral flow. Time series of daily loading (kg/ha) for these three components is shown in Figure 12B, and loadings for
372 percolation, surface water irrigation, and groundwater irrigation are shown in Figure 12C, showing the seasonal trends in
373 applying irrigation water. These results also indicate that much of the salt leaching from the soil profile is due to dissolution of
374 salt minerals. Results also indicate the importance of including salt mass in applied irrigation water, as it accounts for
375 approximately half of salt leaching to the aquifer. Finally, results show the importance of including precipitation-dissolution in
376 the module, as this process is a large component of the salt balance. Without including this process, the module would severely
377 under-predict salt ion concentrations throughout the watershed, demonstrating the need to include each salt ion individually as
378 opposed to modeling salinity as a conservative solute in the system.
379

380

381 **3.3.2.4 Scenarios and Model Guidelines**

382 The effect of initial salt ion concentrations and upstream salt ion mas loading is summarized by the time series charts in
383 Figure 13. For the Rocky Ford and Las Animas gaging sites, a time series of simulated SO_4 (mg/L) and TDS (mg/L) is compared
384 for the following scenarios: uniform initial salt ion concentration ("Original": this refers to the baseline simulation); HRU-
385 variable initial concentration ("Variable IC"); initial concentrations equal to 0 ("Zero IC"); and not accounting for upstream salt
386 ion mass loading at Catlin Dam ("No US Loading").

387 There are only small differences between using uniform or HRU-variable initial concentrations for soil water and
388 groundwater. Any differences are readily resolved during the warm-up period. Hence, to facilitate model use we recommend that
389 uniform initial concentrations be used.

390 Using initial concentrations equal to 0 mg/L has a significant effect, particularly for downstream sites such as Las Animas
391 (Figure 13C, D). For this watershed, salt loading to the streams is principally from groundwater, and if soil water and
392 groundwater are not provided with initial salt ion concentrations, the groundwater salt ion loading to subbasin streams is small
393 compared to the baseline simulation. As downstream flow and in-stream salt loading is effected by groundwater loading, these
394 areas (e.g. Las Animas site) experience the effect more acutely than upstream sites such as Rocky Ford (Figure 13A,B).
395 However, by the end of the simulation (2009), difference between "Zero IC" and "Original" is small. This is shown by the "Diff"
396 time series for each plot. Therefore, if groundwater discharge is a large component of total water yield for the watershed, "Zero
397 IC" should not be used, or a long warm-up simulation period needs to be used.

398 Not including upstream salt ion loading at Catlin Dam has a stronger effect on the Rocky Ford site (Figure 13A,B) than at
399 the outlet (Las Animas) (Figure 13C,D). This is due to Las Animas being much farther downstream, and hence there is much
400 more groundwater salt ion loading to the streams that can make up for the salt not included at the upstream end of the Arkansas
401 River at Catlin Dam. Overall, any point sources of in-stream salt should be added, unless only downstream areas are targeted for
402 baseline simulations and best management practice investigation. The effect of neglecting point sources of in-stream salt
403 decreases as the groundwater loading component of total salt yield increases.

404 The importance of including equilibrium chemistry into the salt transport module is demonstrated by the results shown in
405 Figure 14. The simulated in-stream TDS (mg/L) is shown at the Rocky Ford site (Figure 14A), the Timpas Creek site (B), and
406 the Las Animas site (C), for both the original simulation (red line) and a simulation "No SEC" that does not include the SEC
407 module (black line). The "No SEC" simulation therefore represents a system wherein salt is transported through the stream-
408 aquifer system as a conservative species. Clearly, in-stream concentrations are much too low for the simulation without the SEC
409 module. This is due to the neglect of salt mineral dissolution, which in the actual system transfers salt mass from the soil and
410 aquifer material to soil water and groundwater are thereby increases the loading of salt to the stream network. For this system,
411 and likely most watersheds, equilibrium chemistry must be included to establish the correct magnitude of salt loading and
412 concentrations.

413 **3.3.3 Model Use and Limitations**

414 The salinity module of SWAT differs from other salinity models in that it accounts for salt loading for each major
415 hydrologic pathway in a watershed setting (stream, groundwater, lateral flow, surface runoff, tile drain flow), for each major salt
416 ion, subject to chemical equilibrium reactions (precipitation-dissolution, complexation, cation exchange). As such, it can be used
417 to estimate baseline salt loading within a watershed, and also explore the impact of land management and water management
418 scenarios to mitigate soil salinity, groundwater salinity, and surface water salinity. The model, however, does not simulate
419 physically-based, spatially-distributed groundwater flow and solute transport with an accurate depiction of water table elevation

and groundwater head gradient, and thus the trends in groundwater salt loading to streams may not be accurate (see Figure 9). To overcome this issue, the new salinity module could be incorporated into SWAT-MODFLOW (Bailey et al., 2016), which links SWAT and MODFLOW to simulate land surface and subsurface flow processes, and SWAT-MODFLOW-RT3D (Wei et al., 2018), which includes reactive transport of solutes into SWAT-MODFLOW.

4 Conclusions

This study presents a new watershed-scale salt ion fate and transport model, by developing a salinity module for the SWAT model. The module accounts for salt loading for each major hydrologic pathway in a watershed setting (stream, groundwater, lateral flow, surface runoff, tile drain flow), for each major salt ion (SO_4, Ca, Mg, Na, K, Cl, CO_3, HCO_3). The module also accounts for principal equilibrium chemistry reactions (precipitation-dissolution, complexation, cation exchange). For precipitation-dissolution, five salt minerals ($CaSO_4$, $CaCO_3$, $MgCO_3$, NaCl, $MgSO_4$) have been included. The model was applied and tested in a 732 km^2 irrigated stream-aquifer watershed in southeastern Colorado, along the alluvial corridor of the Arkansas River. Model results are tested against in-stream salt ion concentration, groundwater salt ion concentration, soil salinity, and groundwater salt loading to the Arkansas River.

The model can be used to assess baseline salinity conditions in a watershed and to explore land and water management strategies aimed at decreasing salinization in river basins. Such strategies may include on-farm management, lining irrigation canals to reduce saline canal seepage, dry-drainage practices, and reducing volumes of applied irrigation water. Due to the simulation of soil water salt ion concentrations and SWAT's simulation of crop growth, the salinity module can also be used to investigate the effect of these strategies on crop yield. Although this study applied the model to an irrigated area, the model can be applied to non-irrigated areas as well.

Code Availability

The code consists of the original SWAT files, with 6 additional files for the salinity module. All files are *.f FORTRAN files. The code is available at the following URL: https://github.com/rtbailey8/SWAT_Salinity/tree/v1.0.0 (DOI: 10.5281/zenodo.2541224). An example model input file (salt_input) and example output files are also provided.

Author Contribution

Ryan Bailey wrote the salinity module for SWAT and tested the module for the study region. Saman Tavakoli-Kivi prepared the solution chemistry algorithms for the salinity module. Xiaolu Wei prepared and tested the original SWAT model for the study region, and facilitated use of the new salinity module for the constructed SWAT model.

Competing Interests

The authors declare that they have no conflict of interest.

References

Abbaspour, K.C., Rouholahnejad, E., Vaghefi, S., Srinivasan, R., Yang, H., and Klove, B.: A continental-scale hydrology and water quality model for Europe: Calibration and uncertainty of a high-resolution large-scale SWAT model. Journal of Hydrology 524, 733-752, https://doi.org/10.1016/j.jhydrol.2015.03.027, 2015.

458 Arabi, M., Govindaraju, R.S., Hantush, M.M., and Engel, B.A.: Role of watershed subdivision on modeling the effectiveness of
459 best management practices with SWAT. Journal of the American Water Resources Association 42(2), 513-528,
460 https://doi.org/10.1111/j.1752-1688.2006.tb03854.x, 2006.
461 Bailey, R.T., Wible, T.C., Arabi, M., Records, R.M., and Ditty, J.: Assessing regional-scale spatio-temporal patterns of
462 groundwater-surface water interactions using a coupled SWAT-MODFLOW model. Hydrological Processes 30, 4420-4433,
463 https://doi.org/10.1002/hyp.10933, 2016.
464 Brown, S.C., Versace, V.L., Lester, R.E. and Walter, M.T.: Assessing the impact of drought and forestry on streamflows in
465 south-eastern Australia using a physically based hydrological model, Environmental Earth Sciences, 74(7), 6047-6063,
466 available: http://dx.doi.org/10.1007/s12665-015-4628-8, 2015.
467 Burkhalter, J. P. and Gates, T. K.: Evaluating regional solutions to salinization and waterlogging in an irrigated river valley.
468 Journal of Irrigation and Drainage Engineering, 132(1): 21 – 30, https://doi.org/10.1061/(ASCE)0733-
469 9437(2006)132:1(21), 2006.
470 Dechmi, F. and Skhiri, A.: Evaluation of best management practices under intensive irrigation using SWAT model. Agricultural
471 Water Management 123, 55-64, https://doi.org/10.1016/j.agwat.2013.03.016, 2013.
472 Ficklin, D.L., Luo, Y., Luedeling, E. and Zhang, M.: Climate change sensitivity assessment of a highly agricultural watershed
473 using SWAT, Journal of Hydrology, 374(1-2), 16-29, available: http://dx.doi.org/10.1016/j.jhydrol.2009.05.016, 2009.
474 Frasier, W.M., Waskom, R.M., Hoag, D.L., and Bauder, T.A.: Irrigation Management in Colorado: Survey Data and Findings.
475 Technical Report TR99-5 Agricultural Experiment Station, Colorado State University. Fort Collins, CO, 1999.
476 Gates, T.K., Burkhalter, J.P., Labadie, J.W., Valliant, J.C. and Broner, I.: Monitoring and modeling flow and salt transport in a
477 salinity-threatened irrigated valley, Journal of Irrigation and Drainage Engineering, Vol. 128, No. 2, 88-99,
478 https://doi.org/10.1061/(ASCE)0733-9437(2002)128:2(87), 2002.
479 Gates, T.K, Steed, G.H., Niemann, J.D. and Labadie, J.W.: Data for Improved Water Management in Colorado's Arkansas River
480 Basin, Hydrological and Water Quality Studies, Colorado State University, 2016.
481 Goff, K., M.E. Lewis, M.A. Person, and Konikow, L.F.: Simulated effects of irrigation on salinity in the Arkansas River Valley
482 in Colorado. Ground Water 36:76-86, https://doi.org/10.1111/j.1745-6584.1998.tb01067.x, 1998.
483 Haddeland, I., Heinke, J., Voss, F., Eisner, S., Chen, C., Hagemann, S. and Ludwig, F.: Effects of climate model radiation,
484 humidity and wind estimates on hydrological simulations, Hydrology and Earth System Sciences, 16(2), 305-318, available:
485 http://dx.doi.org/10.5194/hess-16-305-2012, 2012.
486 Jyrkama, M.I. and Sykes, J.F.: The impact of climate change on spatially varying groundwater recharge in the grand river
487 watershed (Ontario), Journal of Hydrology, 338(3-4), 237-250, available: http://dx.doi.org/10.1016/j.jhydrol.2007.02.036,
488 2007.
489 Kaledhonkar, M. J. and Keshari, A. K.: Regional salinity modeling for conjunctive water use planning in Kheri command. J.
490 Irrig. Drain. Eng., 132(4), 389–398, https://doi.org/10.1061/(ASCE)0733-9437(2006)132:4(389), 2006.
491 Kaledhonkar, M.J., Sharma, D.R., Tyagi, N.K., Kumar, A., and Van Der Zee, S.E.A.T.M.: Modeling for conjunctive use
492 irrigation planning in sodic groundwater areas. Agricultural Water Management 107, 14-22,
493 https://doi.org/10.1016/j.agwat.2011.12.023, 2012.
494 Konikow, L.F. and Person, M.: Assessment of long-term salinity changes in an irrigated stream aquifer system. Water Resources
495 Research 21:1611-1624, https://doi.org/10.1029/WR021i011p01611, 1985.

Maringanti, C., Chaubey, I. and Popp, J.: Development of a multiobjective optimization tool for the selection and placement of best management practices for nonpoint source pollution control. Water Resources Research, doi.org/10.1029/2008WR007094, 2009.

Martin, C.A. and Gates, T.K.: Uncertainty of canal seepage losses estimated using flowing water balance with acoustic Doppler devices. Journal of Hydrology 517: 746-761, https://doi.org/10.1016/j.jhydrol.2014.05.074, 2014.

Morway, E.D. and Gates, T.K.: Regional assessment of soil water salinity across an intensively irrigated river valley, Journal of Irrigation and Drainage Engineering, Vol. 138, No. 5, 393-405, https://doi.org/10.1061/(ASCE)IR.1943-4774.0000411, 2012.

Morway, E.D., Gates, T.K. and Niswonger, R.G.: Appraising options to reduce shallow groundwater tables and enhance flow conditions over regional scales in an irrigated alluvial aquifer system. Journal of Hydrology 495, 216-237, https://doi.org/10.1016/j.jhydrol.2013.04.047, 2013.

Mueller Price, J. and Gates, T.K.: Assessing uncertainty in mass balance calculation of river nonpoint source loads. Journal of Environmental Engineering, 134(4), 247-258, https://doi.org/10.1061/(ASCE)0733-9372(2008)134:4(247), 2007.

Napoli, M., Massetti, L, and Orlandini, S.: Hydrological response to land use and climate changes in a rural hilly basin in Italy. CATENA 157, 1-11, https://doi.org/10.1016/j.catena.2017.05.002, 2017.

Neitsch, S.L., J.G. Arnold, J.R. Kiniry, and Williams, J.R.: Soil and Water Assessment Tool Theoretical Documentation, Version 2009. Temple, Tex.: Texas Water Resources Institute Technical Report No. 406, 2011.

National Land and Water Resources Audit, 2001, Australian Government.

Oosterbaan, R. J.: SAHYSMOD (version 1.7a), Description of principles, user manual and case studies, International Institute for Land Reclamation and Improvement, Wageningen, Netherlands, 140, 2005.

Parkhust, D.L. and Appelo, C.A.J.: Description of Input and Examples for PHREEQC Version 3- A Computer Program for Speciation, Batch-Reaction, One-Dimensional Transport, and Inverse Geocehmical Calculations, Chapter 43 of Section A, Groundwater, Book 6, Modeling Techniques, 2013.

Paz-García J., Johannesson, B., Ottosen, L., Ribeiro, A., Rodríguez-Maroto, J.: Computing multi-species chemical equilibrium with an algorithm based on the reaction extents, Computers & Chemical Engineering, Vol: 58 pp: 135-143, https://doi.org/10.1016/j.compchemeng.2013.06.013, 2013.

Rasouli, F., Pouya, A.K., and Šimůnek, J.: Modeling the effects of saline water use in wheat-cultivated lands using the UNSATCHEM model. Irrigation Science 31(5), 1009-1024, https://doi.org/10.1007/s00271-012-0383-8, 2013.

Schoups, G., Hopmans, J.W., Young, C.A., Vrugt, J.A., Wallender, W.W., Tanji, K.K., and Panday, S.: Sustainability of irrigated agriculture in the San Joaquin Valley, California. Proceedings of the National Academy of Sciences of the United States of America, 102(43), 15352-15356, https://doi.org/10.1073/pnas.0507723102, 2005.

Schoups, G., Hopmans, J.W. and Tanji, K.K.: Evaluation of model complexity and space–time resolution on the prediction of long-term soil salinity dynamics, western San Joaquin Valley, California. Hydrological Processes, 20(13), 2647-2668, https://doi.org/10.1002/hyp.6082, 2006.

Šimůnek, J., and Suarez, D.L.: Two-dimensional transport model for variably saturated porous media with major ion chemistry, Water Resources Research, 30(4), 1115-1133, https://doi.org/10.1029/93WR03347, 1994.

Šimůnek, J., M. Šejna, and van Genuchten, M. Th.: The UNSATCHEM Module for HYDRUS (2D/3D) Simulating Two-Dimensional Movement of and Reactions Between Major Ions in Soils, Version 1.0, PC Progress, Prague, Czech Republic, 54 pp, 2012.

Singh, A., and Panda, S.N.: Integrated salt and water balance modeling for the management of waterlogging and salinization; I: Validation of SAHYSMOD, Journal of Irrigation and Drainage Engineering, Vol. 138, 955-963, https://doi.org/10.1061/(ASCE)IR.1943-4774.0000511, 2012.

Susfalk R, Sada D, Martin C, Young MH, Gates T, Rosamond C, Mihevc T, Arrowood T, Shanafield M, Epstein B, and Fitzgerald B.: Evaluation of linear anionic polyacrylamide (LA-PAM) application to water delivery canals for seepage reduction. Desert Research Institute. DHS Publication No. 41245, 2008.

Tavakoli-Kivi, S.: Simulating the fate and transport of salinity species in a semi-arid agricultural groundwater system: model development and application. PhD Dissertation, Dept. of Civil and Environmental Engineering, Colorado State University, Fort Collins, CO, 2018.

Tanji, K. and Kielen, N.: Agricultural drainage water management in arid and semi-arid areas, FAO Irrigation and Drainage Paper 61, Rome, 2002.

Tweed, S., Leblanc, M. and Cartwright, I.: Groundwater-surface water interaction and the impact of a multi-year drought on lakes conditions in South-East Australia, Journal of Hydrology, 379(1-2), 41-53, http://dx.doi.org/10.1016/j.jhydrol.2009.09.043, 2009.

Ullrich, A. and Volk, M.: Application of the Soil and Water Assessment Tool (SWAT) to predict the impact of alternative management practices on water quality and quantity. Agricultural Water Management 96(8), 1207-1217, https://doi.org/10.1016/j.agwat.2009.03.010, 2009.

Umali, D.L.: Irrigation– induced salinity: A growing problem for development and the environment: Technical Paper 215. World Bank, Washington, DC, 1993.

Wagenet, R.J., and Hutson, J.L.: LEACHM-Leaching estimation and chemistry model. Center Environ. Res., Cornell Univ., Ithaca, NY, 1987.

Wei, X., Bailey, R.T. and Tasdighi, A.: Using the SWAT model in intensively managed irrigated watersheds: model modification and application. Journal of Hydrologic Engineering 23(10): 04018044, https://doi.org/10.1061/(ASCE)HE.1943-5584.0001696, 2018.

Zhao, A., Zhu, X., Liu, X., Pan, Y., and Zuo, D.: Impacts of land use change and climate variability on green and blue water resources in the Weihe River Basin of northwest China. CATENA 137, 318-327, https://doi.org/10.1016/j.catena.2015.09.018, 2016.

Zuo, D., Xu, Z., Yao, W., Jin, S., Xiao, P., and Ran, D.: Assessing the effects of changes in land use and climate on runoff and sediment yields from a watershed in the Loess Plateau of China. Science of the Total Environment 544, 238-250, https://doi.org/10.1016/j.scitotenv.2015.11.060, 2016.

Hydrol. Earth Syst. Sci. Discuss., https://doi.org/10.5194/hess-2018-614
Manuscript under review for journal Hydrol. Earth Syst. Sci.
Discussion started: 22 January 2019

Hydrology and Earth System Sciences
Discussions
Open Access
EGU

575
576
577
578
579
580

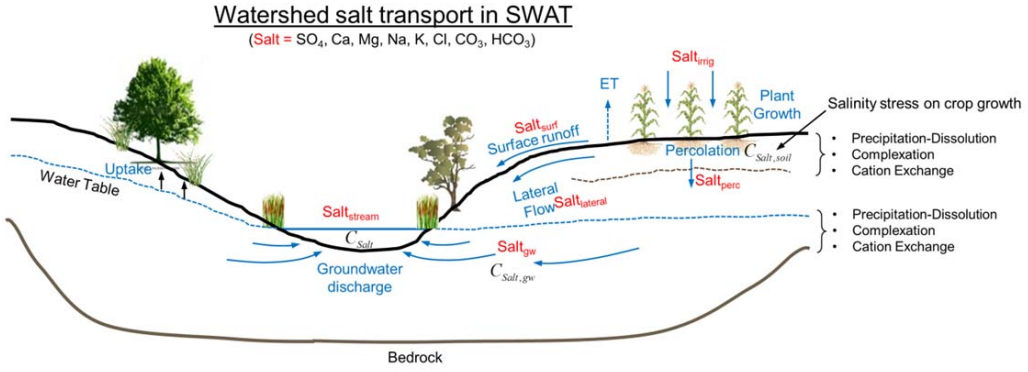

581
582 **Figure 1.** Schematic showing a cross-section of an irrigated stream-aquifer system and the major transport pathways of salt,
583 which consists of the eight major ions of SO_4, Ca, Mg, Na, K, Cl, CO_3, HCO_3. The concentration of each ion is also governed by
584 equilibrium chemistry reactions such as precipitation-dissolution, complexation, and cation exchange within the soil profile and
585 within the aquifer.
586

Hydrol. Earth Syst. Sci. Discuss., https://doi.org/10.5194/hess-2018-614
Manuscript under review for journal Hydrol. Earth Syst. Sci.
Discussion started: 22 January 2019

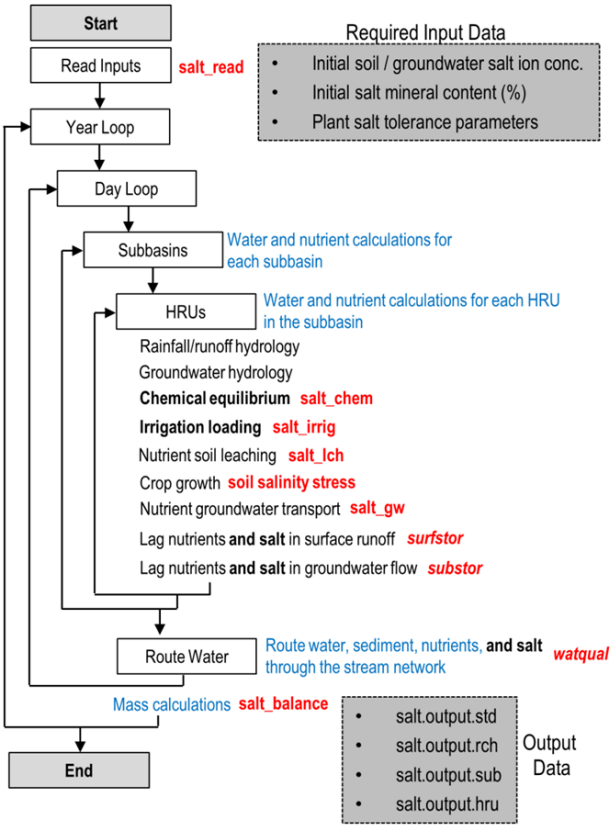

Figure 2. Data flow within the SWAT-Salt modeling code. Boxes and text in black and blue indicate original SWAT loops and subroutines. Text in red indicates either new or modified subroutines for the Salinity module. The required input data for the salinity module is shown in the upper shaded box, whereas the generated output files are shown in the lower shaded box.

Hydrol. Earth Syst. Sci. Discuss., https://doi.org/10.5194/hess-2018-614
Manuscript under review for journal Hydrol. Earth Syst. Sci.
Discussion started: 22 January 2019

Hydrology and Earth System Sciences
Discussions

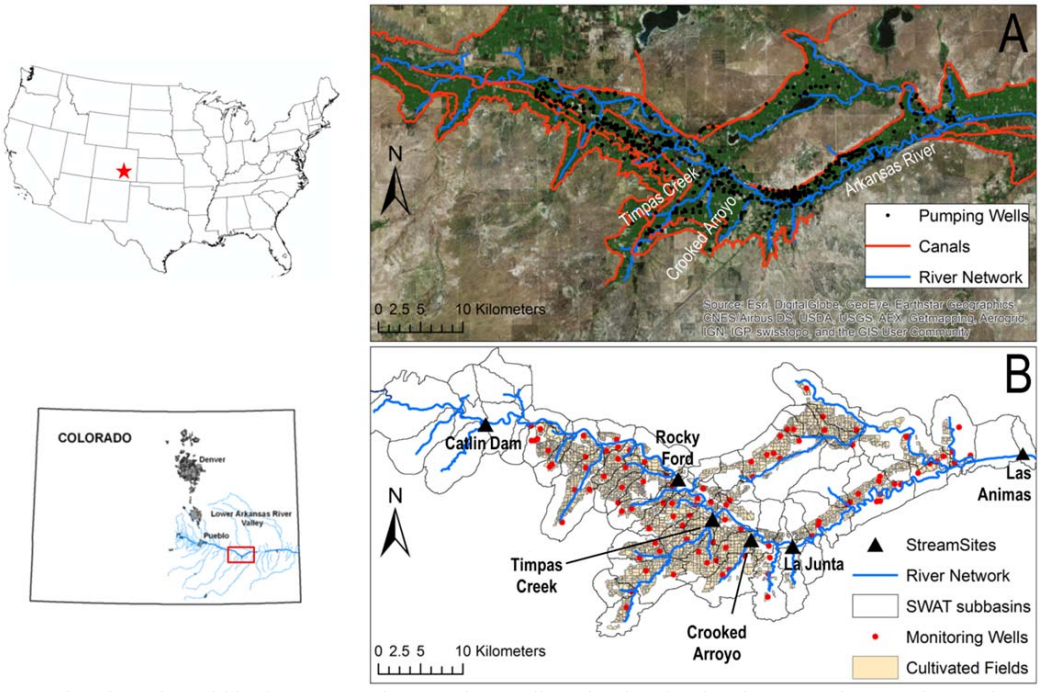

Figure 3. Map of study region within the Lower Arkansas River Valley of Colorado, showing (A) Arkansas River and tributaries, irrigation canals, and pumping wells, and (B) cultivated fields, monitoring wells where groundwater is sampled for salt ions, sampling sites where surface water is sampled for salt ions, and SWAT subbasins.

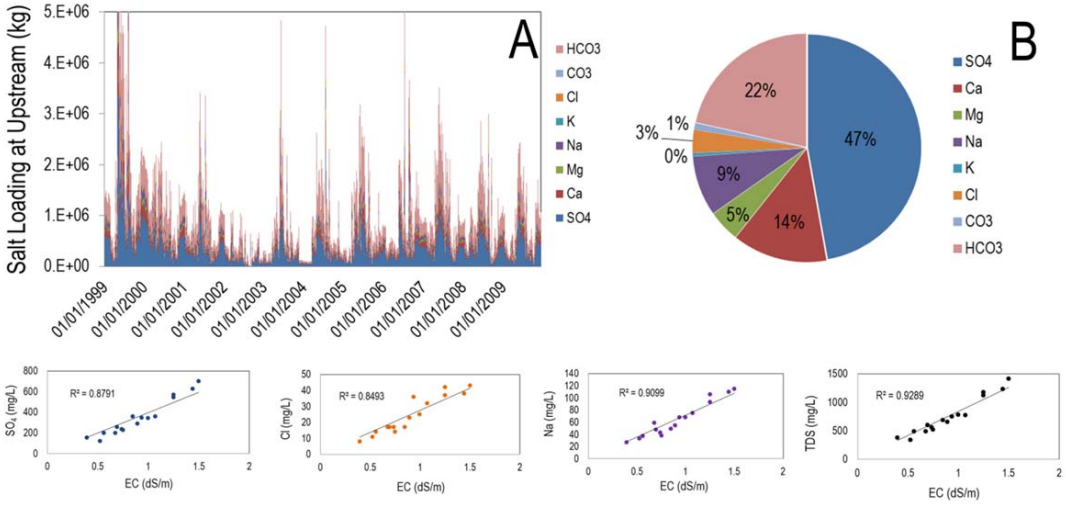

Figure 4. Data summarizing the specified loading of salt (kg/day) at the Catlin Dam gage site, using observed EC (dS/m) and stream discharge (m^3/day) data: (A) daily loading of salt ion, (B) percentage of total salt loading attributed to each salt ion, (bottom charts) example regression plots used to relate EC to salt ion concentration.

Hydrol. Earth Syst. Sci. Discuss., https://doi.org/10.5194/hess-2018-614
Manuscript under review for journal Hydrol. Earth Syst. Sci.
Discussion started: 22 January 2019

Hydrology and Earth System Sciences
Discussions

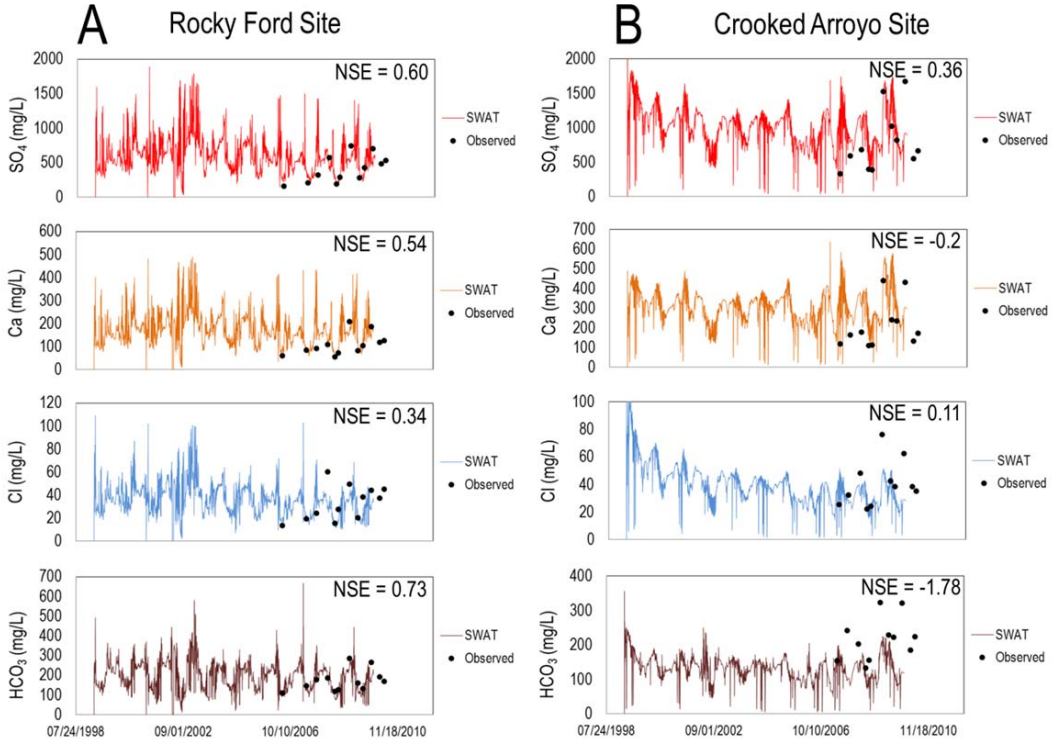

608
609
610 **Figure 5.** Time series of simulated and observed concentration (mg/L) of selected salt ions for the (A) Rocky Ford sampling site
611 along the Arkansas River (see Fig. 3) and the (B) Crooked Arroyo sampling site. The Nash-Sutcliffe model efficiency coefficient
612 (NSE) is shown for each plot.
613

Hydrol. Earth Syst. Sci. Discuss., https://doi.org/10.5194/hess-2018-614
Manuscript under review for journal Hydrol. Earth Syst. Sci.
Discussion started: 22 January 2019

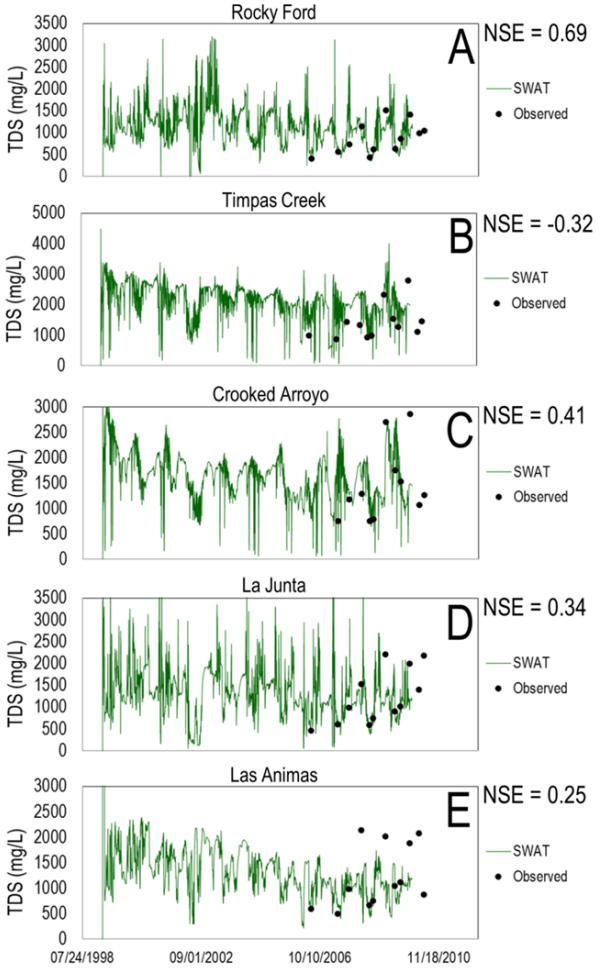

Figure 6. Simulated and observed total dissolved solids (TDS) (mg/L) in the five stream sampling sites along the Arkansas River (A, D, E), and two tributaries (B, C). See Fig. 3 for locations. TDS is the summation of the concentration of the 8 salt ions. The Nash-Sutcliffe model efficiency coefficient (NSE) is shown for each plot.

Hydrol. Earth Syst. Sci. Discuss., https://doi.org/10.5194/hess-2018-614
Manuscript under review for journal Hydrol. Earth Syst. Sci.
Discussion started: 22 January 2019

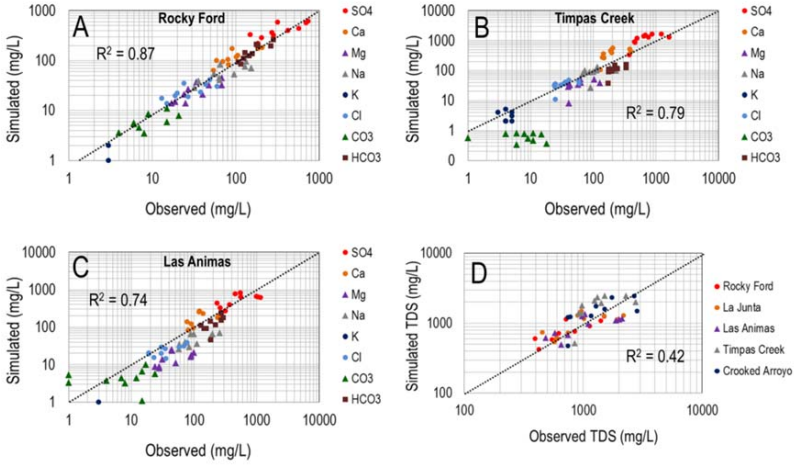

Figure 7. Log-log plots of observed vs. simulated salt ion concentration for the (A) Rocky Ford, (B) Timpas Creek, and (C) Las Animas surface water sampling sites. (D) shows the comparison of TDS for the five sites.

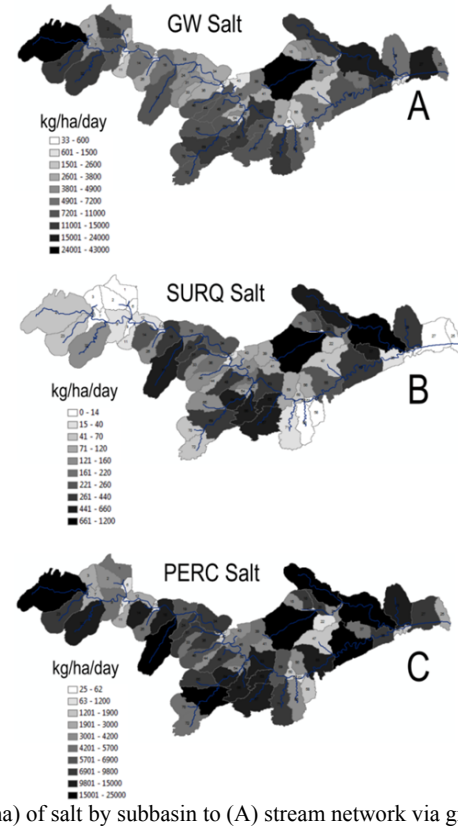

Figure 8. Average daily loading (kg/ha) of salt by subbasin to (A) stream network via groundwater discharge, (B) stream network via surface runoff, (C) groundwater via soil percolation.

Hydrol. Earth Syst. Sci. Discuss., https://doi.org/10.5194/hess-2018-614
Manuscript under review for journal Hydrol. Earth Syst. Sci.
Discussion started: 22 January 2019

Hydrology and Earth System Sciences
Discussions

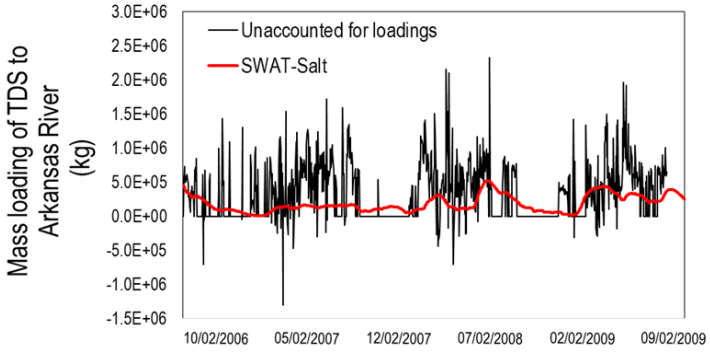

631
632 **Figure 9.** Simulated daily mass loading of TDS (kg) to the Arkansas River via groundwater discharge for the SWAT model with
633 uniform initial salt concentrations. Results from a salt mass balance calculation on the Arkansas River also are plotted, showing
634 the unaccounted for TDS loadings (groundwater, surface runoff, small inflows) in the Arkansas River.
635
636
637
638
639

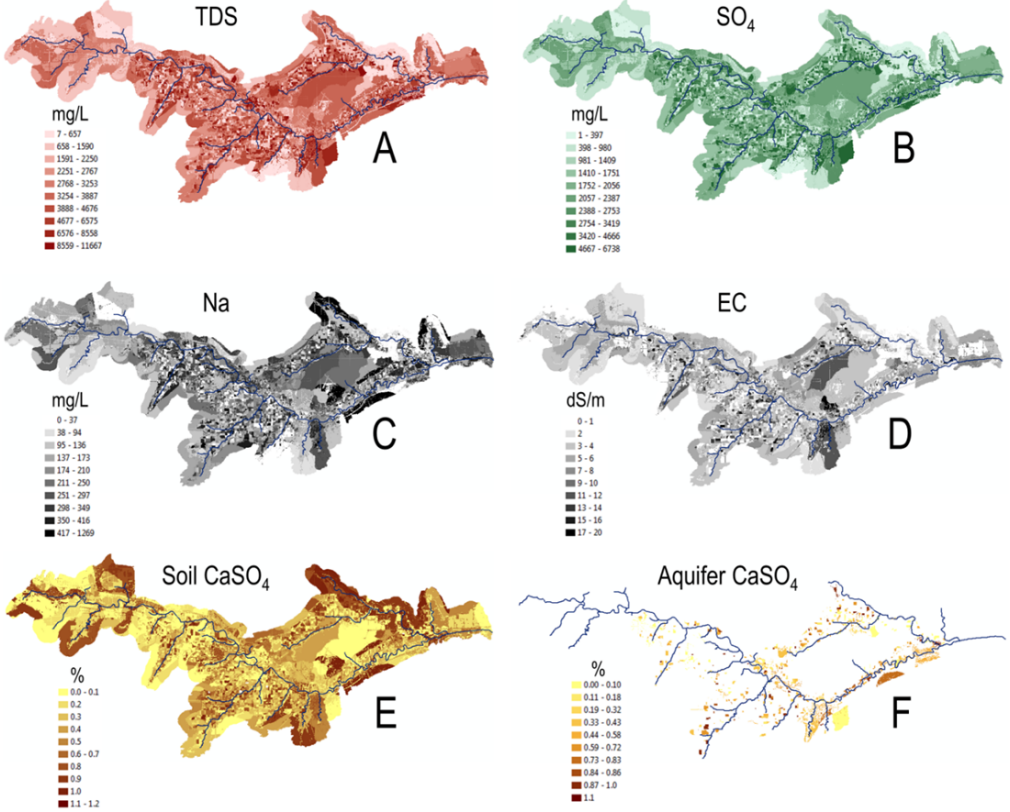

640
641 **Figure 10.** HRU average concentration over the 2006-2009 simulation period for (A) groundwater TDS (mg/L), (B) groundwater
642 SO_4 (mg/L), (C) groundwater Na (mg/L), and (D) soil water electrical conductivity EC (dS/m). (E) and (F) show percentage of
643 soil bulk volume and aquifer bulk volume, respectively, that is $CaSO_4$, near the end of the simulation in May 2010.
644
645
646

Hydrol. Earth Syst. Sci. Discuss., https://doi.org/10.5194/hess-2018-614
Manuscript under review for journal Hydrol. Earth Syst. Sci.
Discussion started: 22 January 2019

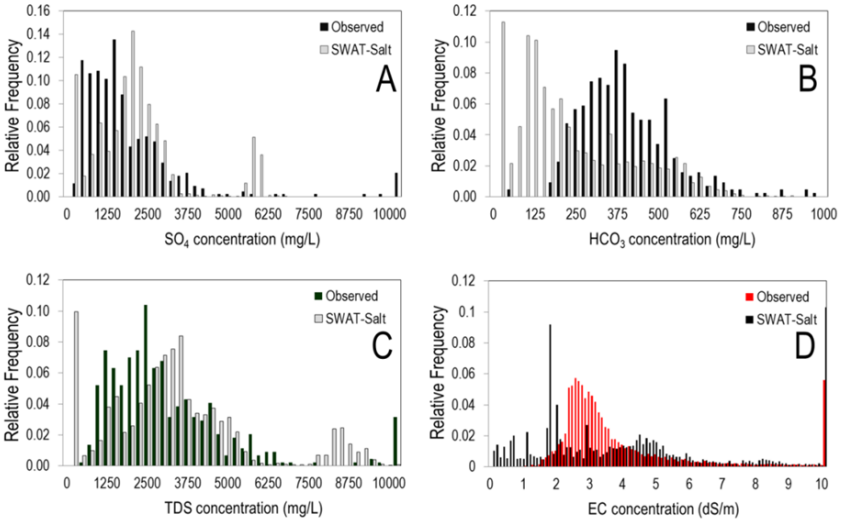

Figure 11. Relative frequency plots of simulated and observed values of (A) SO_4 groundwater concentration, (B) HCO_3 groundwater concentration, (C) TDS groundwater concentration, and (D) EC soil water concentration. Simulated values are taken from each HRU of the SWAT simulation, on days for which observed values are available.

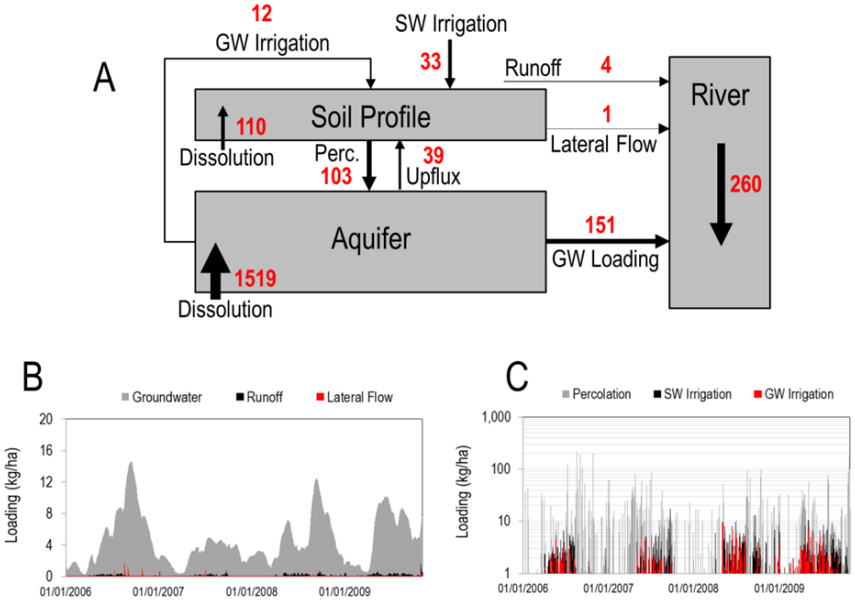

Figure 12. Magnitude of salt balance components in the watershed model for TDS, showing (A) relative salt flux between soil storage compartments in the watershed for each salt transport pathway; (B) daily loading (kg/ha) of salt in groundwater, surface runoff, and lateral flow to streams; and (C) daily loading (kg/ha) of salt in percolation water (from bottom of soil profile to the aquifer), irrigation derived from irrigation canals, and irrigated derived from groundwater pumping.

Hydrol. Earth Syst. Sci. Discuss., https://doi.org/10.5194/hess-2018-614
Manuscript under review for journal Hydrol. Earth Syst. Sci.
Discussion started: 22 January 2019

Hydrology and Earth System Sciences
Discussions

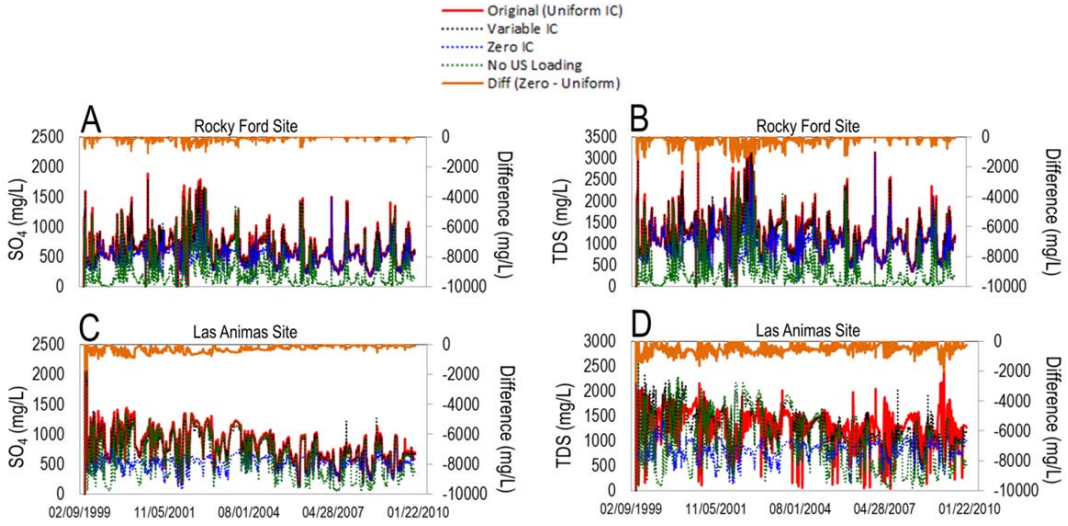

Figure 13. Simulated in-stream SO_4 and TDS concentration (mg/L) at the Rocky Ford Site and the Las Animas Site along the Arkansas River for four scenarios: uniform initial conditions (IC) of salt soil water and groundwater concentrations, corresponding to the original simulation; variable IC; IC = 0; and no upstream loading of salt at the Catlin Dam site. Also show is the difference between the IC = 0 scenario and the original scenario.

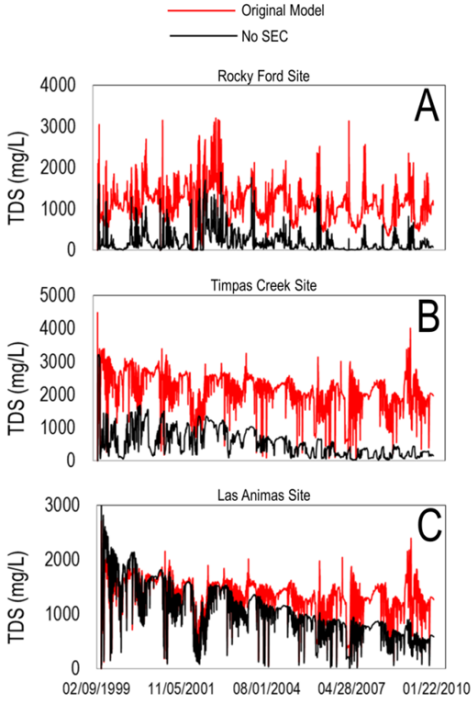

Figure 14. Simulated in-stream TDS concentration (mg/L) at the (A) Rocky Ford Site, (B) Timpas Creek Site, and (C) Las Animas Site for the original simulation (red line) and a simulation without including equilibrium chemistry (SEC module) (black line).

Hydrol. Earth Syst. Sci. Discuss., https://doi.org/10.5194/hess-2018-614
Manuscript under review for journal Hydrol. Earth Syst. Sci.
Discussion started: 22 January 2019

Hydrology and Earth System Sciences
Discussions
Open Access
EGU

676 **Table 1.** Groups and Species included in the Salinity Equilibrium Chemistry (SEC) module for SWAT.

Group	Species
Aqueous Species	Ca^{2+}, Mg^{2+}, Na^{+}, K^{+},SO_4^{-2}, CO_3^{2-}, HCO_3^{-},Cl^{-}
Solid Species	CaSO4,CaCO3,MgCO3,NaCl, MgSO4
Complexed Species	$CaSO_4^0$, $MgSO_4^0$, $CaCO_3^0$, $CaHCO_3^+$, $MgCO_3^0$, $MgHCO_3^+$, $NaSO_4^-$, KSO_4^-, $NaHCO_3^0$, $NaCO_3^0$
Exchanged Species	Ca, Mg, Na, K

677
678
679
680
681
682
683
684
685
686
687
688
689
690
691
692
693
694
695
696
697
698
699
700
701
702
703
704
705
706
707
708
709
710
711

Hydrol. Earth Syst. Sci. Discuss., https://doi.org/10.5194/hess-2018-614
Manuscript under review for journal Hydrol. Earth Syst. Sci.
Discussion started: 22 January 2019

Hydrology and Earth System Sciences
Open Access
Discussions

712 **Table 2.** Summary statistics for observed (monitoring well) and simulated (SWAT) salinity concentrations in groundwater.
713

	Maximum (mg/L)		Average (mg/L)	
Species	Observed	Simulated	Observed	Simulated
Na	2606	1269	402	187
Ca	767	2234	353	653
Mg	1019	497	191	78
K	85	277	4	9
SO_4	6510	6738	1878	2058
CO_3	42	8	2	0
HCO_3	2362	1828	410	225
Cl	1803	480	95	65
TDS	13007	11667	3334	3276

714
715